IEEE Access
Multidisciplinary | Rapid Review | Open Access Journal

Received June 22, 2018, accepted August 24, 2018, date of publication August 31, 2018, date of current version September 21, 2018.

Digital Object Identifier 10.1109/ACCESS.2018.2868059

Fabric Defect Detection Using Salience Metric for Color Dissimilarity and Positional Aggregation

KAIBING ZHANG, YADI YAN, PENGFEI LI, JUNFENG JING, XIUPING LIU, AND ZHEN WANG
College of Electronics and Information, Xi'an Polytechnic University, Xi'an 710048, China

Corresponding author: Kaibing Zhang (xihua_0169@163.com)

This work was supported in part by the National Natural Science Foundation of China under Grant 61471161, in part by the Key Project of the Natural Science Foundation of Shaanxi Province under Grant 2018JQ1017, in part by the Doctoral Startup Foundation of Xi'an Polytechnic University under Grant BS1314 and Grant BS1616, in part by the Natural Science Foundation of Hubei Province under Grant 2016CFB395, in part by the Hubei Provincial Department of Education Outstanding Youth Scientific Innovation Team Support Foundation under Grant T201410, in part by the Youth Talent Promotion Project of the Shaanxi Association for Science and Technology under Grant 20180115, in part by the Natural Science Foundation of Shaanxi Provincial Department of Education under Grant 15JK1305, and in part by the Young Science and Technology Star Project of the Shaanxi Innovation Talent Promotion Plan under Grant 2018KJXX-038.

ABSTRACT In this paper, inspired by an inherent characteristic of human visual system capable of recognizing salient regions from a complicated scene, we treat a defective region as a salient region in fabric images. A novel fabric defect detection method, which is based on saliency metric for color dissimilarity and positional aggregation, is proposed. In the method, the RGB color space of a given fabric image is first converted into the CIE L*a*b color space for feature representation. Then, the color dissimilarity and the positional distance between similar patches are jointly used to measure the defective values. To improve the contrast between the defective region and the non-defective region, a multi-scale analysis scheme performed on the pyramid images of the input fabric image is applied to calculate the defective values. Finally, the obtained defect map image is further enhanced by a certain threshold regarding to the obtained defective values. Thorough experimental results on several types of fabric images indicate the effectiveness of the newly proposed method.

INDEX TERMS Color dissimilarity, defect map, fabric defect detection (FDD), K-nearest neighbor (KNN), multi-scale.

I. INTRODUCTION

In textile industry, it is crucial to control the quality of fabric products. Traditionally, the fabric defect detection (FDD) is conducted by manual manner. However, the manual methods are fundamentally high cost and low efficiency [1]. In particular, it has been shown that manual detection methods only can achieve forty percent to sixty percent of detection rate [2]; moreover, the accuracy of this kind is prone to be influenced by emotional and subjective factors of workers [3]. Therefore, to gear up the high quality demand of fabric products, it is necessary to develop an automatic approach to FDD based on machine vision and image processing technology.

Since the 1970s, the automatic FDD techniques have gained great attention and many approaches have been proposed in the research field from different perspectives [4], [5]. Generally speaking, the existing FDD approaches can be roughly divided into three categories, i.e., statistic-based methods, spectrum-based methods, and model-based methods [6]–[8].

The statistical approaches typically extract statistical features of fabric images by using different statistics, and the obtained feature parameters are used to distinguish non-defective regions from defective regions [9]. For example, Liu *et al.* [10] utilized edge detection and projection profile analysis for fabric defects detection; Reddy *et al.* [11] applied gray level co-occurrence matrix and binary pattern schemes to establish automated similarity identification and defect detection model; Çelik *et al.* [12] proposed to use linear filtering and morphological operations to detected fabric defect. In [13] a fuzzy inductive reasoning based on image histogram statistic variables is designed for defect detection. This kind of methods can efficiently locate larger defect areas which are obviously different from the background [14]. Nevertheless, they fail to detect small defects or the defects similar to the background [15].

In contrast, the model-based methods usually train a special-purpose model to estimate the textural feature parameters of fabric images. For example, Zhang *et al.* [16]

employed a multi-resolution Markov Random Field to segment jacquard warp-knitted fabric in the wavelet domain; Bu *et al.* [17] presented a defect detection method by using auto-regressive spectral analysis and support vector data description; Wang *et al.* [18] adopted the fractal model to predict the permeability of stain fabric. Due to the model-dependence of these methods, their detection performance highly relies on the selected model parameters. Moreover, the presumed model is insufficient to describe complicated textural structures of fabric images. In additional, learning model parameters is time-consuming, which limits their potential applications in practice [19].

Unlike the two aforementioned types of methods, the spectrum methods carry out fabric defect analysis in the spectrum domain based on the spectrogram. For example, Malek *et al.* [20] utilized fast Fourier transform (FFT) and cross-correlation to examine the structure regularity features of fabric images for defect detection; Kuo *et al.* [21] utilized the wavelet packets and the neural classifier for classifying non-defective and defective fabric images; Jing *et al.* [22] developed a genetic algorithm to design an optimal Gabor filter to match the texture information of non-defective fabric image and applied the obtained optimal Gabor filter to accomplish defect detection. Although these methods have been shown particularly effective for the repeat textures and unpatterned fabric images based upon time-frequency analysis and multi-scale analysis, the results are greatly affected by the suitable selection of frequency-domain filters and the proper configuration of related parameters [23].

In recent years, many other sparse representation based methods and deep learning-based methods are getting popular for FDD. For example, Tong *et al.* [24] presented a nonlocal sparse representation approach for FDD; Liu *et al.* [25] used sparse representation of main local binary pattern for FDD; Li *et al.* [26] suggested a fisher criterion-based deep learning algorithm for deformable patterned FDD; Wang *et al.* [27] proposed a convolutional neural network-based defect detection model for product quality control, showing robust and fast performance; Ren *et al.* [28] employed a generic deep-learning-based approach for automated surface inspection. Despite the promising results obtained by the aforementioned methods, the detection performance of them depends on the learning of a large number of defective fabric images.

Up to now, many FDD methods for various applications have been proposed from different viewpoints. However, there is still much room to further improve the accuracy and the efficiency of FDD when processing the fabric images with complicated textures [29]. In recent years, simulating human visual attention mechanism for visual information analysis has gained much attention and shown great success in many fields such as object detection [30], objection segmentation [31], and image compression [32]. The study shows that human visual system (HVS) is able to quickly focus on some salient goals and prioritize them in the observation of a complex scene. With this inherent ability, human eyes can quickly and accurately locate a salient region based on the mechanism of visual attention [33], [34].

Roughly speaking, the current salient detection algorithms can be divided into two categories [35], namely the bottom-up and the top-down methods. One of the most classic bottom-up methods was proposed in [36], where intensity, color, and orientation features are combined to generate the expected saliency map. Following the Itti's model, a variety of saliency detection methods have been proposed in different aspects. For example, Hou and Zhang [37] adopted spectral residual (SR) approach to saliency detection; Guan and Gao [38] employed visual attention mechanism in the wavelet domain to segment fabric defect regions; Liu *et al.* [39] developed a FDD algorithm based on feature representation of local binary pattern (LBP) and context-based local texture saliency analysis, showing promising performance.

The success of saliency research and applications inspire us to target defect detection via saliency analysis. The main idea behind this method is twofold. One is that the colors of the local defective regions in a fabric image visually differ from those of the non-defective regions; the other is that the defective regions are often grouped together within a small region rather than spread throughout the whole image. The fact prompts us that in contrast to the non-defective regions, the defective regions are visually salient [40]. Based on the above observation, we propose to integrate two features of color dissimilarity and positional aggregation to achieve FDD. Specifically, if the color distance between two local image patches is large and inversely the positional distance between them is small, the pixel can be seen as a potential defective region. In summary, the contributions of the paper are the following three aspects.

1) We elaborate on the fabric defect analysis in terms of the insight of saliency detection, where the defective value of a pixel is jointly measured by the color distance and the positional distance.
2) We enhance the contrast the non-defective and defective regions by multi-scale dissimilarity analysis, resulting in a reliable and robust result on FDD.
3) Extensive experiments carried out on different types of fabric images indicate that the proposed method can achieves state-of-art results by comparing with other predecessors.

The rest of this paper is organized as follows. Section II provides a brief overview of the proposed method. In Section III we present the details of our method. Section IV presents the experimental results and assesses the effectiveness of our method in comparing with other state-of-the-art competitors in literature. Final Section V concludes this paper.

II. OVERVIEW OF THE PROPOSED METHOD

Figure 1 illustrates the flow chart of the proposed method. The main steps are comprised of three parts: 1) dissimilarity of color features, 2) similarity of positional distance, and 3) generation of the defect map.

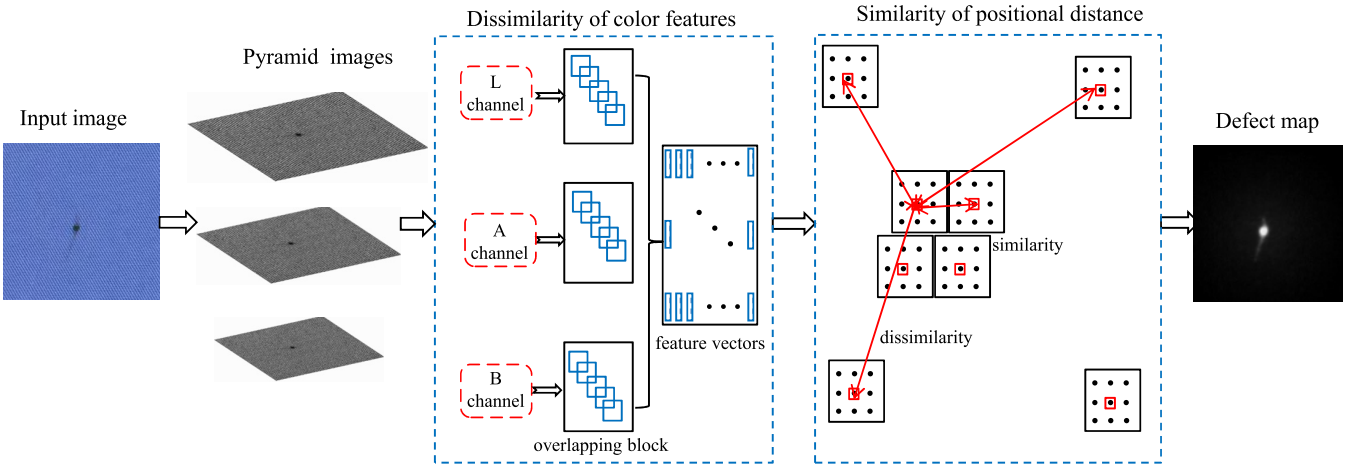

FIGURE 1. The flow chart of proposed FDD method.

1) **Dissimilarity of color features**: We first build the pyramid images of the input fabric image and then transform them into the CIE L*a*b color space. Next each color channel is divided into patches and the corresponding patches are concatenated together for feature representation. Finally the Euclidean distance is computed to measure the dissimilarity of color features.
2) **Similarity of positional distance**: We calculate the Euclidean distance between two given patches to measure the positional similarity.
3) **Generation of defect map**: The color dissimilarity and the positional distance of similar neighbors are jointly used to compute the defective values and generate the defect map.

III. THE PROPOSED DEFECT DETECTION METHOD

In this paper, the four principles of context-aware saliency detection suggested in [41] are followed up to accomplish the task of defect detection. The major idea behind the proposed method is that the region different from fabric background texture should obtain higher defective possibility while the regions frequently occurring should be effectively suppressed. Furthermore, the defective pixels should be grouped together and not be spread all over the image. In the following section, we will detail the proposed defect detection method from three parts. In the first subsection, the CIE L*a*b color feature to represent local image patches is presented. Next how to generate the defect map for defect detection is described in the second subsection. Finally, we summarize the proposed method.

A. REPRESENTATION OF COLOR FEATURES

One of the most key problems of the FDD is how to represent the feature of fabric images. In the research field of FDD, textural feature, intensity feature, orientation feature, and color feature, are widely used to characterize the difference between non-defective pixels and defective pixels. Considering that the color feature shows higher robustness and less dependence on the size and orientation of the images than other features, in this paper we utilize color features of fabric images to compare the dissimilarity of image patches.

Since the CIE L*a*b color space is based on HVS, it has been shown powerful representation ability of visual information and widely used in various image analysis tasks [42]–[44]. In this paper we also follow the same research direction and use the CIE L*a*b color space to represent local image patches. To represent the features of local image patches, we first convert a color fabric image from the RGB space to the CIE L*a*b color space. Next three channels are respectively divided into a set of 7×7 local patches. Finally, the extracted local patches in three components are concatenated together into a 147-dimensional feature vector for defect analysis. To improve the computational efficiency, we use the principal component analysis (PCA) to reduce the dimension of the original color features to represent each image patch, where 95 percent of energy is preserved. It is experimentally shown that the reduced features can significantly improve the computational efficiency without degrading the defect detection accuracy. Figure 2 demonstrates the major steps of feature representation in the proposed method.

Let $\mathbf{p}_i$ and $\mathbf{p}_j$ be the features at the i-th and j-th positions in the image to be detected. The color similarity between $\mathbf{p}_i$ and $\mathbf{p}_j$ is measured by the Euclidean distance $d_{color}(\mathbf{p}_i, \mathbf{p}_j)$, which is denoted as below:

$$d_{color}(\mathbf{p}_i, \mathbf{p}_j) = \left\| color(\mathbf{p}_i) - color(\mathbf{p}_j) \right\|_2^2, \tag{1}$$

where $color(\mathbf{p}_i)$ is the color feature vector of the i-th patch and $color(\mathbf{p}_j)$ is the color feature vector of the j-th patch, respectively. Note that the i-th pixel is possibly defective when $d_{color}(\mathbf{p}_i, \mathbf{p}_j)$ is higher than others. In practice, to evaluate the defective possibility of a pixel, there is no need to compare it with all other image patches. For each image patch $\mathbf{p}_i$, we only select K nearest neighbors $\{\mathbf{p}_k\}_{k=1}^{K}$ from the obtained feature set. In our experiment, we empirically set

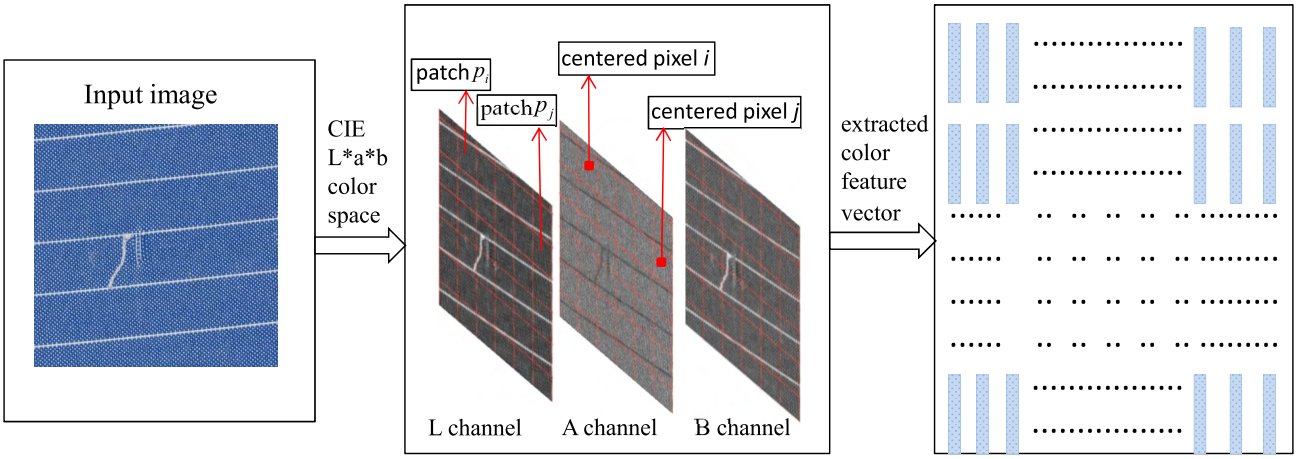

FIGURE 2. Illustration of feature representation.

$K = 64$ and normalize the Euclidean distance $d_{color}(\mathbf{p}_i, \mathbf{p}_j)$ to the range [0, 1] by all the pixel values divided by 255.

B. SIMILARITY OF POSITIONAL DISTANCE

Besides the dissimilarity of color feature, we also take the positional distance of patches into account. According to the basic principle of human visual attention, the defective region may be salient and appear within one or a few small ranges. That is to say, the non-defective region tends to occur many times throughout the image; while the defective regions are typically grouped together within a relatively smaller range. Thus, we can say that a patch $\mathbf{p}_i$ is a possible defective region if its similar neighbors are near enough. By contrast, a patch $\mathbf{p}_i$ does not belong to a defective region when its similar patches are far away from it. In this paper, we denote $d_{distance}(\mathbf{p}_i, \mathbf{p}_j)$ as the positional distance between the i-th patch and the j-th patch, respectively. For the positional distance between two similar patches, we normalize it by the larger dimension of the width and height of the input fabric image.

C. GENERATION OF DEFECT MAP

In order to measure the defective value of a pixel, we combine the color features and the distance information to define the dissimilarity of two compared patches as follows.

$$d(\mathbf{p}_i, \mathbf{p}_j) = \frac{d_{color}(\mathbf{p}_i, \mathbf{p}_j)}{1 + c \cdot d_{distance}(\mathbf{p}_i, \mathbf{p}_j)} \tag{2}$$

where $c = 3$ is a constant coefficient to adjust the positional distance, $d_{distance}(\mathbf{p}_i, \mathbf{p}_j)$ is the Euclidean distance of the patch $\mathbf{p}_i$ and the patch $\mathbf{p}_j$. Based on Eq. (2), we can see that the pixel i is a defective pixel when its color is highly different from others and its positional distance is nearby enough.

To achieve a reliable result, intuitionally a given patch should be compared with all other patches in the image. Obviously, the way is computationally intensive. In the experiment, we have found that it is sufficient enough to consider the K most similar patches to measure the dissimilarity. The strategy is based on the fact that when the K most similar patches are significantly different from the given patch, all other patches in the image are certainly different from the patch. According to the above consideration, we apply the dissimilarity metric in Eq. (2) to search the K most similar patches and compute the defective value of the pixel i at scale r as below:

$$s_i^r = 1 - \exp\left\{-\frac{1}{K}\sum_{k=1}^{K} d(\mathbf{p}_i^r, \mathbf{p}_k^r)\right\}, \tag{3}$$

where s_i^r is the defective value of the pixel i at scale r, $\mathbf{p}_k^r$ is the k-th patch at scale r in the similar neighbors consisting of the $K(K = 64)$ most similar patches.

In fabric images, the non-defective pixels are likely to have similar patches at multiple scales. By contrast, the defective pixels only appear at a few scales rather than at all of the scales. As a result, the similar patterns at multi-scales can be considered to enhance the contrast between the defective region and the non-defective region. This can be achieved by searching similar neighbors from the pyramid images of an input fabric image. When the multi-scale dissimilarity analysis is made to calculate defective values, Eq. (3) is reformulated as below:

$$s_i^r = \left[1 - \exp\left\{-\frac{1}{K}\sum_{k=1}^{K} d(\mathbf{p}_i^r, \mathbf{p}_k^{r_k})\right\}\right], \tag{4}$$

where $\mathbf{p}_k^{r_k}$ represents the similar patches at four scales $r_k = \left[r, \frac{4}{5}r, \frac{1}{2}r, \frac{3}{10}r\right]$. The procedure of generating defect map by fusing the results of multiple scales is illustrated in Figure 3. As shown in Figure 3, we first perform defect detection at four different scales and then compute the mean of defective values regarding these four scales. It is worth noticing that the defective map s_i^r at a lower scale is required to upscale to the original size by Bicubic interpolation algorithm. The mean of

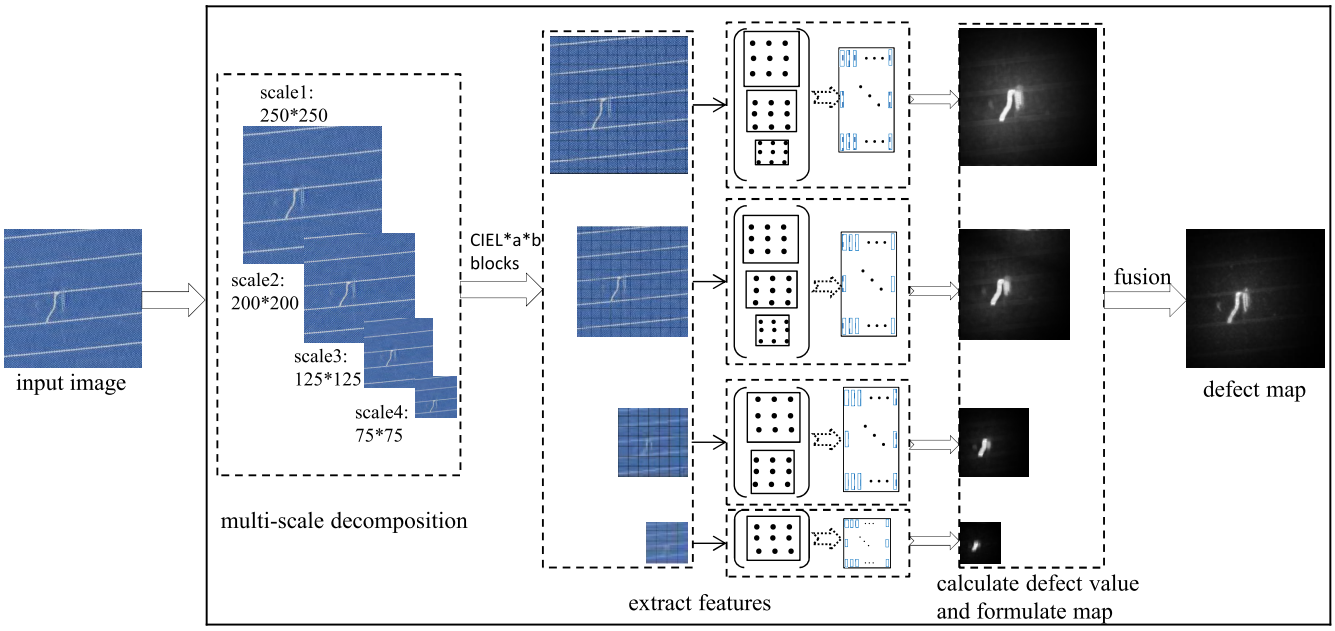

FIGURE 3. Multi-scales defect detection.

defect values at the i-th pixel is defined as below:

$$\hat{s}_i = \frac{1}{M} \sum_{r \in R} s_i^r, \tag{5}$$

where $R = \left\{r, \frac{4}{5}r, \frac{1}{2}r, \frac{3}{10}r\right\}$ and $M = 4$. In terms of Eq. (5), the larger $\hat{s}_i$ means the larger dissimilarity to the other patches.

To achieve more obvious detection result, a better way is to enhance higher defect values and suppress the lower defect values. This can be mimicked by using the mechanism of human visual attention proposed in [33]. According to Lin's method [34], the contrast of the defect values can be strengthened by comparing them with a fixed threshold value (0.8 in our paper), where the value larger than 80 percent of the maximal value of the obtained defect map is regarded as an attended local region. Then each pixel outside the attended regions is reweighted in terms of the Euclidean distance to the closest attended pixel, i.e.,

$$\hat{s}_i = \bar{s}_i \left(1 - d_{foci}\left(i\right)\right), \tag{6}$$

where $d_{foci}(i)$ is the distance between the pixel i and the closest center of the attended pixel, which is normalized to the range [0, 1].

D. SUMMARY OF THE PROPOSED ALGORITHM

In summary, the proposed defect detection algorithm for a given fabric image is presented in Algorithm 1.

Algorithm 1 The Proposed FDD Algorithm

Input: A defect fabric image $\mathbf{X}$.
Output: The final defective map.

1: Convert $\mathbf{X}$ from the RGB color space to the CIE L*a*b color space.
2: Generate the pyramid images of three color channels at four scales.
3: Divide the pyramid images into 7×7 patches with one overlapping pixel.
4: Calculate the normalized Euclidean distance $d_{color}(\mathbf{p}_i, \mathbf{p}_j)$ using Eq. (1).
5: Calculate the normalized positional distance $d_{distance}\left(\mathbf{p}_i, \mathbf{p}_j\right)\big)$.
6: Apply multi-scale dissimilarity analysis to calculate defective values using Eq. (4).
7: Aggregate defective values at multi-scales using Eq. (5).
8: Enhance defective map using Eq. (6).

IV. EXPERIMENTAL RESULTS AND ANALYSIS

A. EXPERIMENTAL DATASET

To validate the effectiveness of the proposed method, we use 130 fabric defect images collected from practical product to compare the performance of different methods. The test images cover a wide range of different defect types such as hole defect, stain defect, thrum defect, warp defect, and weft defects. Some fabric defect samples are listed in Figure 4.

B. EXPERIMENTAL CONFIGURATION

Given an RGB color fabric image, we first convert it into the CIE L*a*b color space. Then each color component is divided into 7×7 image patches with one overlapping pixel at the adjacent patches. The scale number r is set to 4 for multiple scale analysis. All the experiments are conducted on a PC with an Intel(R) Core processor 3.2GHz and 6GB RAM memory. The algorithm is implemented on MATLAB R2014a programming platform.

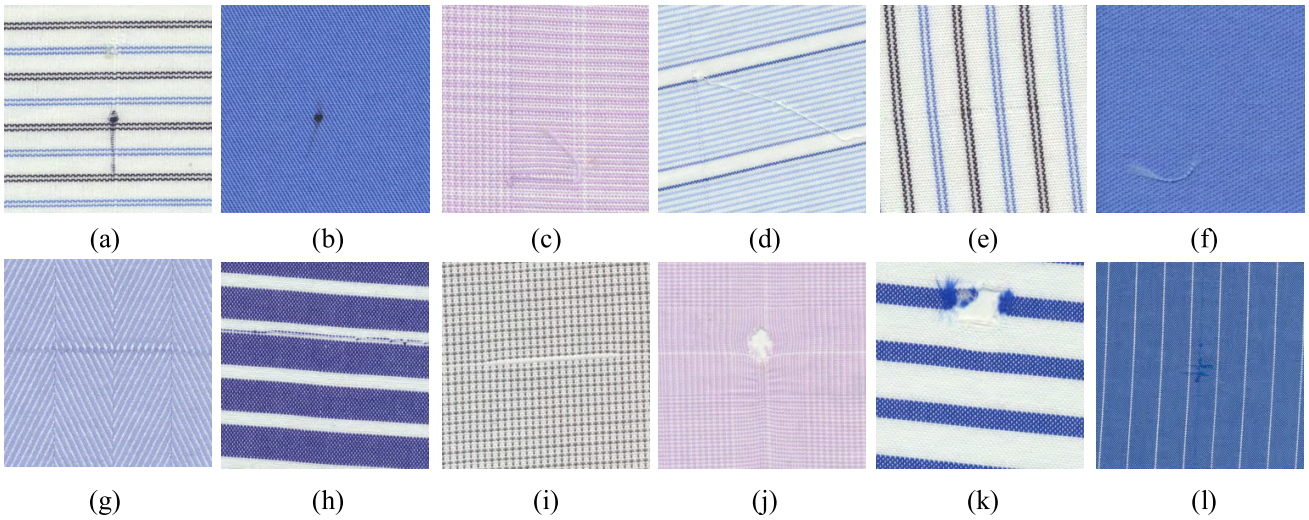

FIGURE 4. Some typical fabric defect samples. (a) and (b) are stain; (c) is broken warp; (d) and (e) are loss; (f) is thrum; (g) is ribbon yarn; (h) is harness balk; (i) are ribbon yarn; (j) and (k) is hole; (l) is loose crane.

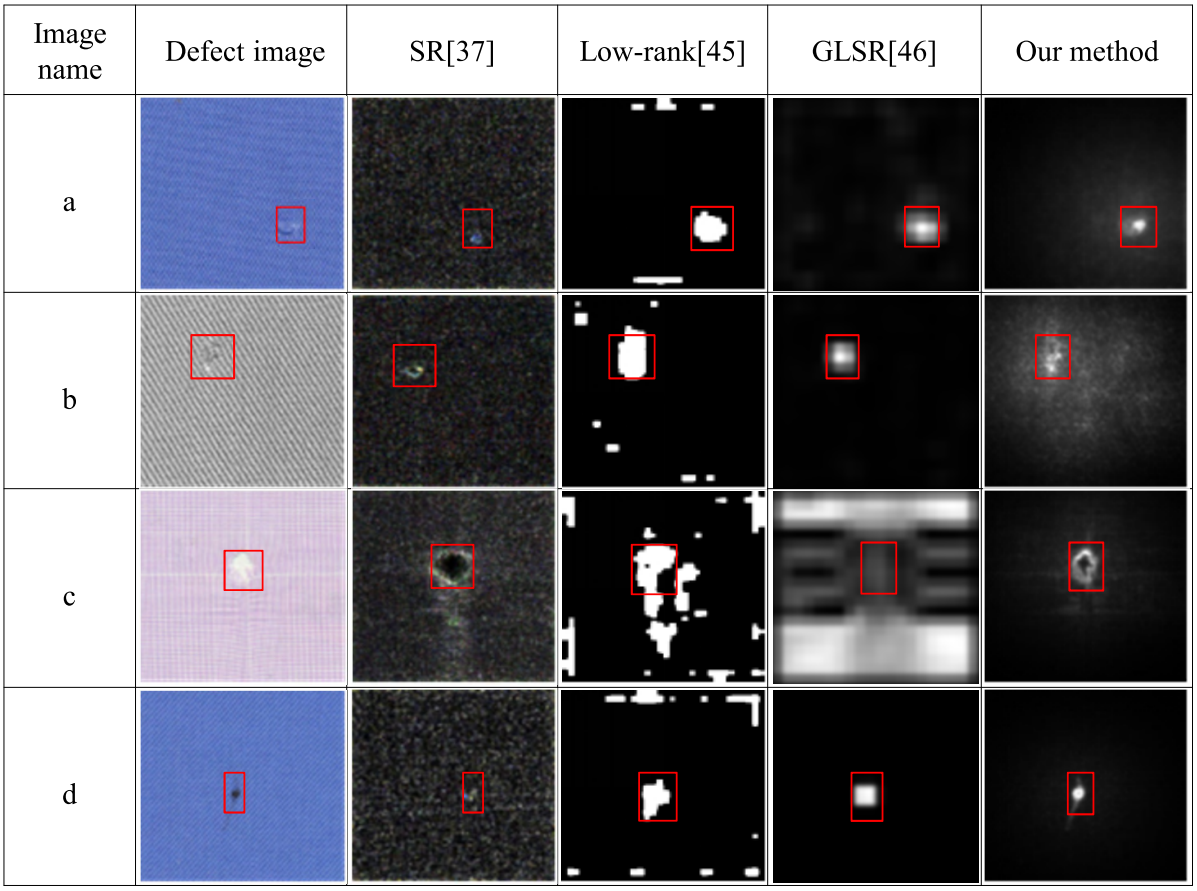

FIGURE 5. Comparison of non-patterned fabric defective images. (a) and (b) are cotton ball; (c) is holes; (d) is stains. From the second left column to the right column are non-patterned fabric defective images, the results of SR-based method [37], the results of Low-rank representation [45], the results of GLSR-based method [46], and the results of proposed method, respectively.

C. EXPERIMENTAL RESULTS

In this subsection, we evaluate the effectiveness of the proposed FDD algorithm by comparing with other three state-of-art methods. The compared methods include SR-based method [37], low-rank representation based method [45], and the prior knowledge guided least squares

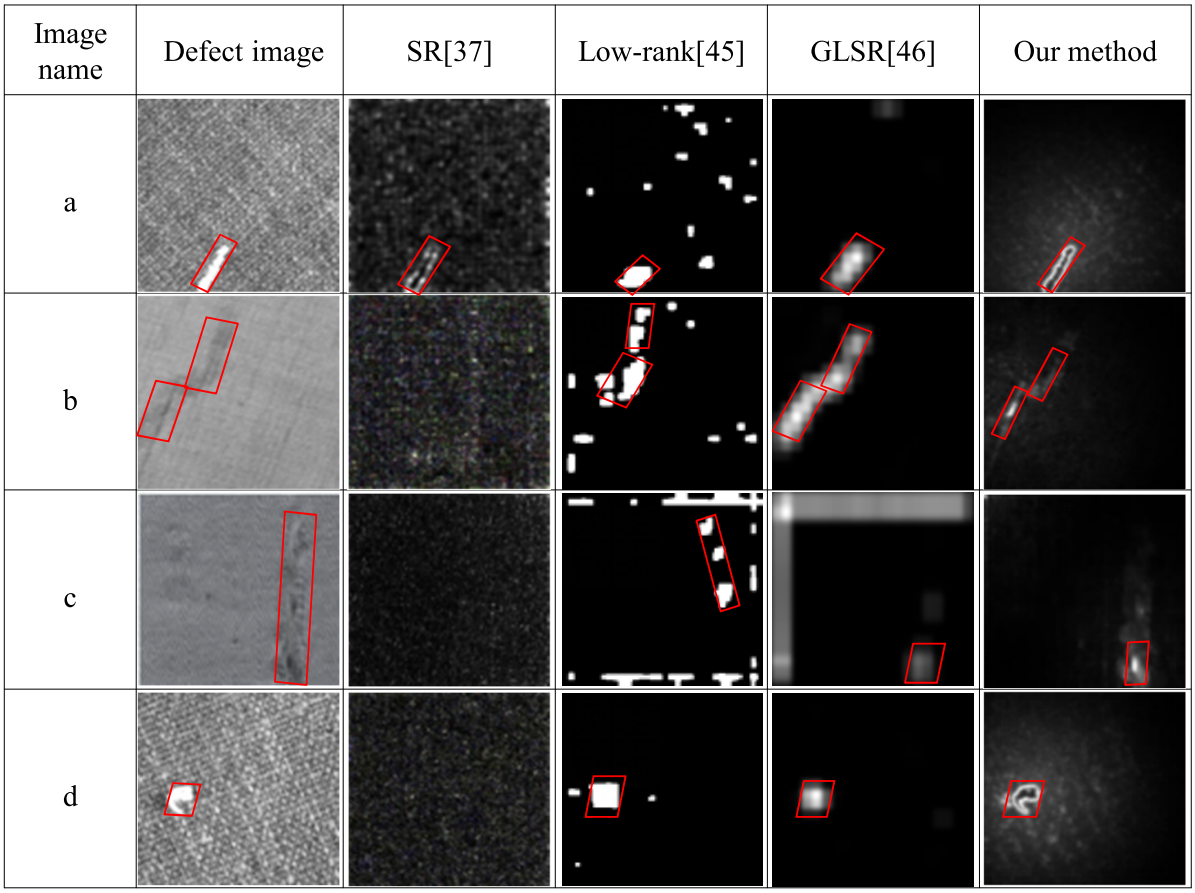

FIGURE 6. Comparison of non-patterned gray fabric defective images. (a) is scratches; (b) is stains; (c) is belt yarn; (d) is cotton ball. From the second left column to the right column are gray fabric defective images, the results of SR-based method [37], the results of low-rank representation based method [45], the results of GLSR-based [46], and the results of proposed method, respectively.

regression (GLSR) based method [46]. The SR-based method constructs the corresponding defect map by analyzing the log-spectral of an input image in spectral domain. The low-rank representation based method decomposes the data matrix into two parts: a low-rank part and a sparse part. The GLSR-based is also a low-rank based method, which learns a simple and effective prior to guide least squares regression for FDD. The obtained sparse part is regarded as the expected defect region. To validate the defect detection capability for different types of fabric images, we select three categories of textural structures to perform our experiment, which they are non-patterned, gray, and patterned fabric structures.

1) RESULTS ON NON-PATTERNED, GRAY, AND PATTERNED FABRIC IMAGES

In Figure 5, we compare the defect detection results of four representative non-patterned fabric images. Based on the results in the figure, the SR-based method can locate the position of defect region, but the obtained results are not contrastive enough. The low-rank representation based method can effectively detect most defects. However, the method is clumsy at locating insignificant defects in the non-patterned fabrics and is prone to introducing lots of noticeable noisy results. The GLSR-based method can detect mostly defects of non-pattered and gray images, but not outstanding for the pattered image. By contrast to the above competitors, the newly proposed can successfully locate all the defect regions, leading to the best results. The second experiment is tested on a set of gray fabric images as shown in Figure 6. As demonstrated in the figure, we can find that our method also enables the best result among the compared approaches. This is because that the defect region is fundamentally salient from the perspective of visual attention mechanism, so the proposed method can effectively target the defect detection.

To further validate the effectiveness of the proposed method, we carry out another experiment on patterned fabric images with complicated textures and different colors. The defect detection on the pattered fabric image is challenging for the compared methods. Figure 7 presents the results. As illustrated, we can find that the other competitors cannot successfully obtain the desired results. Contrastively, our method can suppress the regular patterns and efficiently distinguish the defect region with singular colors and irregular

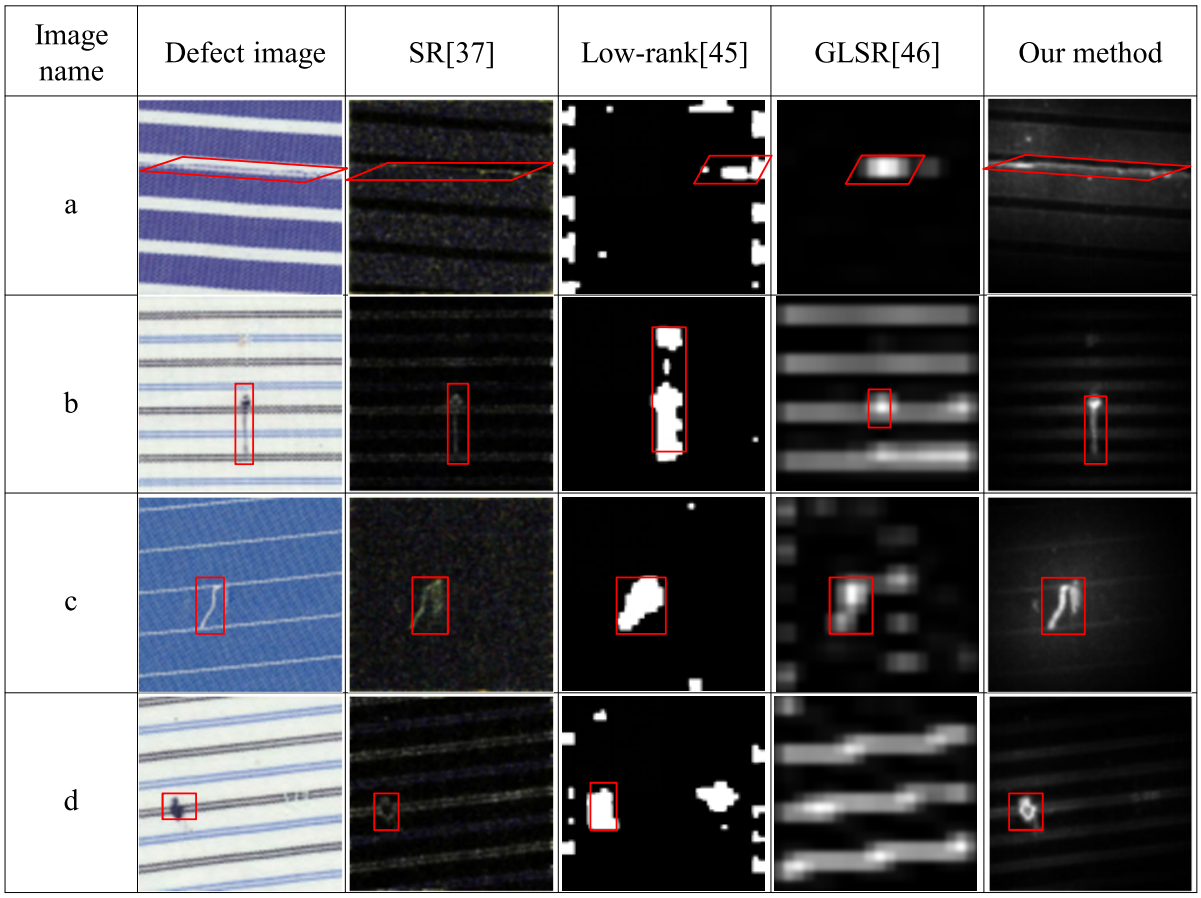

FIGURE 7. Comparison of patterned fabric defective images. (a) is harness balk; (b) is stains; (c) is floating thread; (d) is stains and flushing. From the second left column to the right column are patterned defective images, the results of SR-based method [37], the results of low-rank representation based method [45], the results of GLSR-based [46], and the results of proposed method, respectively.

textures from the non-defective region with regular textural structures.

2) COMPARISON OF DETECTION RATE

In this subsection, we further evaluate the performance of the proposed method by comparing the detection rate (DR) with the competitors. The experiment is carried out on four types of lattice, gray, stripe, and plates fabric images. Each type consists of 20 images with different defects including holes, stains, belt yarn, cotton ball, and so on. The DR is employed to evaluate the performance of detection performance, which is defined as below.

$$DR = \frac{DN}{TN} \times 100\%, \tag{7}$$

where DN is the number of accurate detection, and TN is the number of total fabric images.

Table 1 tabulates the DR of four different types of fabric defect images. As the results presented in the table, we can see that the proposed method achieves the best performance on the two types of Lattice and Plates images, reaching 85% and 90%, respectively. For two types of Gray and Stripe image, the DRs of our method are 90% and 75%, respectively,

TABLE 1. Comparison of detection rate.

Methods	SR-based[37]	Low-rank[45]	GLSR-based[46]	Our method
Lattice	20%	50%	60%	85%
Gray	40%	40%	90%	90%
Stripe	70%	55%	75%	75%
Plates	50%	35%	65%	90%

which are comparable to GLSR-based method but superior to the SR-based method [37] and low-rank based method [45]. Although the overall DR of our method is the best performance, we also notice that the proposed method shows relatively lower DR on Lattice and Stripe fabric images. This is because that defects in Lattice and Stripe fabric images are similar to the backgrounds and the Lattice and Stripe regions are easily regarded as saliency regions, leading to mistake detection.

D. INFLUENCE OF SIMILAR NEIGHBORS

In the proposed method, an important parameter is the number of similar neighbors K used for calculating the dissimilarity in Eq. (3). In this subsection, we verify the reasonability

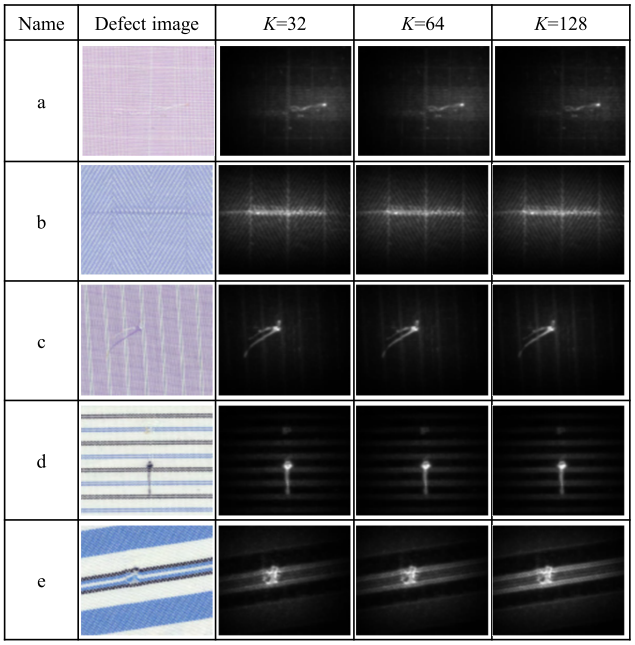

FIGURE 8. Defect detection results influenced by different similar neighbors. (a) and (c) are the detection results of floating thread; (b) is the detection result of ribbon yarn; (d) is the detection result of stains; (e) is the detection result of holes. From left to right: the names of fabric defective images, the defective images, and the defect maps with $K = 32$, $K = 64$, and $K = 128$, respectively.

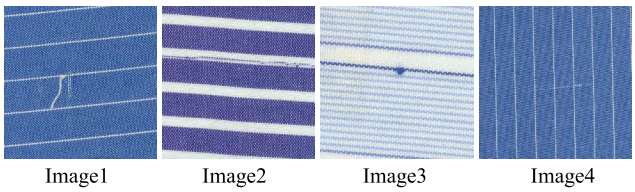

FIGURE 9. Four test images for evaluating the CPU time.

of selecting the K most similar neighbors rather than all other patches in the image. Figure 8 displays the results obtained from three different numbers of neighbors, i.e., $K = 32$, 64, and 128, respectively. Based on the results we can see that there are no significant differences when different numbers of similar neighbors are used for the defect detection. Nevertheless, we also notice that more similar neighbors are helpful to achieve more robust and more contrastive result. However, too many similar neighbors would result in much computational cost, which does not benefit real-time applications. To study how the number of similar neighbors affects the computational time in the proposed method, we select four fabric images of the size is 250×250 shown in Figure 9 to compare the CPU time by setting the similar neighborhood size K to 32, 64, and 128, respectively. As demonstrated in Figure 10, more similar neighbors will cost more CPU time. To take a tradeoff between the computational time and the detection accuracy, we suggest selecting medium-sized similar neighbors ($K = 64$) in the proposed framework.

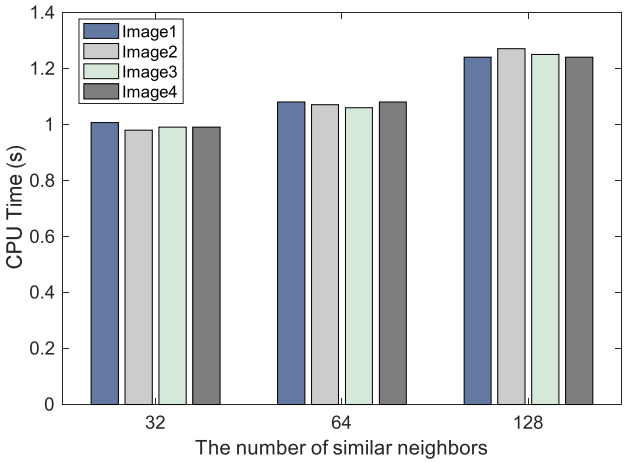

FIGURE 10. Comparison of the CPU time for four different fabric images shown in Figure 9.

E. INFLUENCE OF THE SIZE OF IMAGE PATCH

In the experiment, we also find that the size of image patch fundamentally impacts the detection result. The smaller size may tend to more similar neighbors which are not similar at all, leading to too larger defect regions. While too larger size could result in finding the less similar neighbors, leading to inaccurate results. To probe a suitable image patch size, we choose three different sizes of image patches, i.e., 3×3, 7×7, and 11×11, to compare their performance. The contrastive results are shown in Figure 11 and Table 2, respectively.

TABLE 2. The saliency values and the CPU running time.

Image Name	Patch Size	3×3	7×7	11×11
a	Saliency Values	0.048	**0.149**	0.252
	CPU Time (s)	0.73	**1.41**	2.42
b	Saliency Values	0.051	**0.137**	0.227
	CPU Time (s)	0.71	**1.18**	2.66
c	Saliency Values	0.056	**0.154**	0.251
	CPU Time (s)	0.71	**1.17**	2.40
d	Saliency Values	0.053	**0.150**	0.242
	CPU Time (s)	0.72	**1.18**	2.68
e	Saliency Values	0.044	**0.126**	0.208
	CPU Time (s)	0.57	**1.04**	3.03

Figure 11 displays the results using different image patch sizes. Based on the Figure 11, we can find that the sizes of 3×3 (see the third column) and 11×11 (see the fifth column) produce a relatively larger defect region in comparing with the original images. By contrast, the obtained results from the size of 7×7 (see the fourth column) are more faithful to the original defect as showed at the fourth column in Figure 11.

Furthermore, we compare the saliency values and the CPU time varying with different sizes of image patches to select an optimal size of patch. Moreover, we notice that the larger size of patch may result in larger saliency value as shown in Table 2. From the results tabulated in the table, in comparison to the results obtained from 3×3 and 7×7 image patches, we can observe that the patch size of 11×11 can

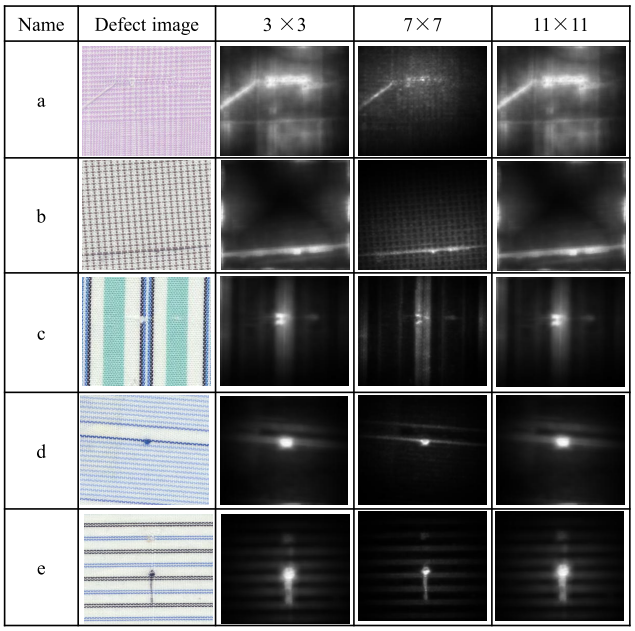

FIGURE 11. Defect detection results influenced by different sizes of image patches. (a) is the results of cracked warp; (b) is the results of missing waft; (c) is the results of belt yarn; (d) is the results of Knot; (e) is the results of stains. From left to right: the names of images, the defective images, and the defect maps obtained by using the patch sizes of 3 × 3, 7 × 7, and 11 × 11, respectively.

achieves the top level saliency value but takes more CPU time. To take a tradeoff between the computational time and the detection performance, we suggest using the medium-size patch, i.e., 7×7 in the proposed FDD for efficient detection.

F. EFFECTIVENESS OF MULTI-SCALE FUSION

In this subsection, we validate the effectiveness of multi-scale analysis strategy by comparing the results from single-scale and multi-scale. The compared results from four single scales (e.g., $r = 1$, $r = 2$, $r = 3$, and $r = 4$) and the fused results towards four scales are shown in Figure 12. In terms of the figure, we can find that the fused results are the best among the compared results. The fact tells us that similar patches at multiple scales can improve both the accuracy and the contrast of resultant defect maps.

G. ROBUSTNESS AGAINST GAUSSIAN NOISE

In practical applications, the noise is not avoidable for FDD. In order to validate the robustness against noise of the proposed method, the additive Gaussian noise are added into the test images for defect detection. Figure 13 demonstrates the experimental result by the centered Gaussian noise with the standard deviation of 0.02. Based on the results, we can find that the proposed method does well on the defect detection of noisy fabric images and achieves comparable results to the images without any noise. This is because the color dissimilarity and positional aggregation of K similar neighbors are considered in the proposed approach, which benefits to suppress the noise influence on the defect detection.

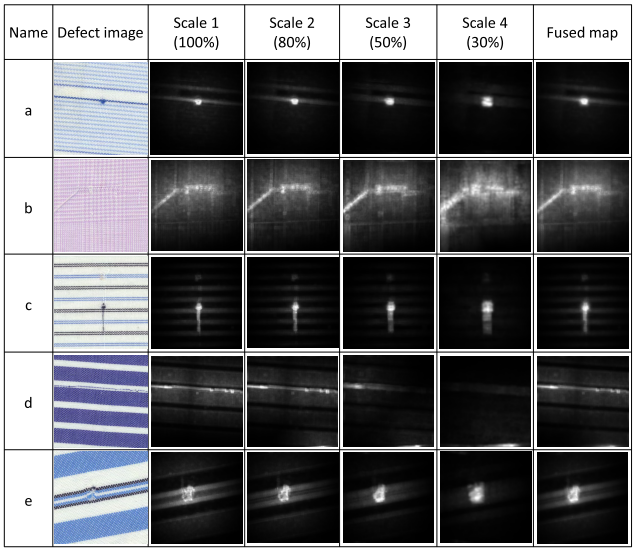

FIGURE 12. Comparison of defect detection using multi-scale fusion. (a) is the detection results of Knot; (b) is the detection results of cracked warp; (c) is the detection results of belt yarn; (d) is the detection results of harness balk; (e) is the detection results of hole. From left to right: the name of image, the defect maps at scale 1(100%), the defect maps at scale 2(80%), the defect maps at scale 3(50%), the defect maps at scale 4(30%), the fused defect maps of four scales, respectively.

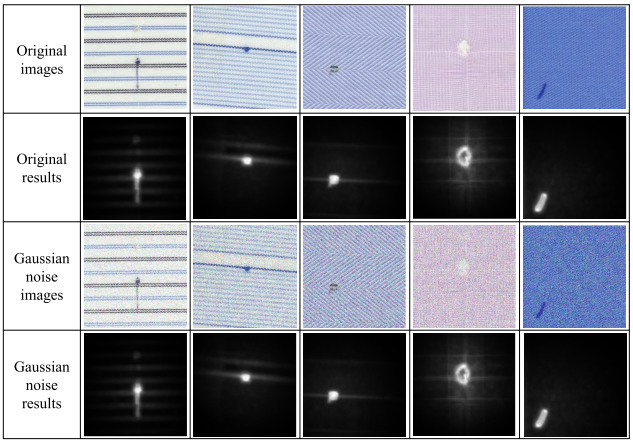

FIGURE 13. Defect detection results on the fabric images with and without the Gaussian noise. The first row is input images without noise; the second row is the detection results at the first row; the third row is the images with the Gaussian noise; the fourth row is the detection results at the third row.

V. CONCLUSIONS

This paper has presented a novel FDD method based on the mechanism of visual attention. In the proposed method, an effective and robust saliency metric which incorporates the color dissimilarity and the positional aggregation is proposed for FDD. Extensive experimental results demonstrate that 1) the proposed method can achieve more accurate defect detection than other state-of-art competitors, 2) the proposed method show good robustness on the fabric images with different textural structures different types of defects, and 3) the multi-scale similarity introduced in the proposed method can

effectively improve the contrast between the non-defective region and the defective region. Despite the effectiveness of the proposed method for fabric images with complicated patterns, it is still clumsy at accurately detecting the defects in the motif and box-patterned fabric images. In the future, we will continue to elaborate on integrating multi-view feature learning algorithms [47], structural kernel analysis [48], and sparse representation [49] to further improve the performance of the proposed method.

ACKNOWLEDGMENT

The authors would like to thank the Associate Editor and the anonymous reviewers for their constructive and insightful comments on this paper.

REFERENCES

[1] K. Srinivasan, P. H. Dastoor, P. Radhakrishnaiah, and S. Jayaraman, "FDAS: A knowledge-based framework for analysis of defects in woven textile structures," *J. Textile Inst.*, vol. 83, no. 3, pp. 431–448, 1992.
[2] K. Schicktanz, "Automatic fault detection possibilities on nonwoven fabrics," in *Proc. Melliand Textilberichte Int. Textile Rep.*, 1993, pp. 294–295.
[3] Y. F. Zhang and R. R. Bresee, "Fabric defect detection and classification using image analysis," *Textile Res. J.*, vol. 65, no. 1, pp. 1–9, 1995.
[4] A. Kumar, "Computer-vision-based fabric defect detection: A survey," *IEEE Trans. Ind. Electron.*, vol. 55, no. 1, pp. 348–363, Jan. 2008.
[5] H. Y. T. Ngan, G. K. H. Pang, and N. H. C. Yung, "Automated fabric defect detection—A review," *Image Vis. Comput.*, vol. 29, no. 7, pp. 442–458, 2011.
[6] R. G. Saeidi, M. Latifi, S. S. Najar, and A. G. Saeidi, "Computer vision-aided fabric inspection system for on-circular knitting machine," *Textile Res. J.*, vol. 75, no. 6, pp. 492–497, 2005.
[7] S. Priya, T. A. Kumar, and V. Paul, "A novel approach to fabric defect detection using digital image processing," in *Proc. Int. Conf. Signal Process., Commun., Comput. Netw. Technol.*, Jul. 2011, pp. 228–232.
[8] Y. H. Zhang, C. W. M. Yuen, W. K. Wong, and C. W. Kan, "An intelligent model for detecting and classifying color-textured fabric defects using genetic algorithms and the Elman neural network," *Textile Res. J.*, vol. 81, no. 17, pp. 1772–1787, 2011.
[9] D. Yapi, M. S. Allili, and N. Baaziz, "Automatic fabric defect detection using learning-based local textural distributions in the contourlet domain," *IEEE Trans. Autom. Sci. Eng.*, vol. 15, no. 3, pp. 1014–1026, Jul. 2018.
[10] Z. Liu, J. Huang, and C. Li, "Skew detection of fabric images based on edge detection and projection profile analysis," in *Foundations of Intelligent Systems*. Berlin, Germany: Springer, 2011, pp. 483–488.
[11] R. O. K. Reddy, B. E. Reddy, and E. K. Reddy, "Classifying similarity and defect fabric textures based on GLCM and binary pattern schemes," *Int. J. Inf. Eng. Electron. Bus.*, vol. 5, no. 5, pp. 25–33, 2013.
[12] H. I. Çelik, L. C. Dülger, and M. Topalbekiroğlu, "Fabric defect detection using linear filtering and morphological operations," *Indian J. Fibre Textile Res.*, vol. 39, no. 3, pp. 254–259, 2014.
[13] Y. Ye, "Fabric defect detection using fuzzy inductive reasoning based on image histogram statistic variables," in *Proc. 6th Int. Conf. Fuzzy Syst. Knowl. Discovery*, Aug. 2009, pp. 191–194.
[14] C.-Y. Wen, S.-H. Chiu, W.-S. Hsu, and G.-H. Hsu, "Defect segmentation of texture images with wavelet transform and a co-occurrence matrix," *Textile Res. J.*, vol. 71, no. 8, pp. 743–749, 2001.
[15] M. A. Selver, V. Avşar, and H. Özdemir, "Textural fabric defect detection using statistical texture transformations and gradient search," *J. Textile Inst.*, vol. 105, no. 9, pp. 998–1007, 2014.
[16] Y. Zhang, G. Jiang, J. Yao, and Y. Tong, "Intelligent segmentation of jacquard warp-knitted fabric using a multiresolution Markov random field with adaptive weighting in the wavelet domain," *Textile Res. J.*, vol. 84, no. 1, pp. 28–39, 2014.
[17] H.-G. Bu, X.-B. Huang, J. Wang, and X. Chen, "Detection of fabric defects by auto-regressive spectral analysis and support vector data description," *Textile Res. J.*, vol. 80, no. 7, pp. 579–589, 2010.
[18] G. Wang, H. Chen, S. Lv, and X. Zhao, "Research on permeability of satin fabrics based on fractal theory," *J. Reinforced Plastics Compos.*, vol. 34, no. 5, pp. 377–387, 2015.
[19] P. Li, H. Zhang, J. Jing, R. Li, and J. Zhao, "Fabric defect detection based on multi-scale wavelet transform and Gaussian mixture model method," *J. Textile Inst.*, vol. 106, no. 6, pp. 587–592, 2015.
[20] A. S. Malek, J. Y. Drean, L. Bigue, and J. F. Osselin, "Optimization of automated online fabric inspection by fast Fourier transform (FFT) and cross-correlation," *Textile Res. J.*, vol. 83, no. 3, pp. 256–268, 2013.
[21] C.-F. J. Kuo, C.-Y. Shih, C.-C. Huang, and Y. M. Wen, "Image inspection of knitted fabric defects using wavelet packets," *Textile Res. J.*, vol. 86, no. 5, pp. 553–560, 2016.
[22] J. Jing, P. Yang, P. Li, and X. Kang, "Supervised defect detection on textile fabrics via optimal Gabor filter," *J. Ind. Textiles*, vol. 44, no. 1, pp. 40–57, 2014.
[23] K. Hanbay, M. F. Talu, and O. F. Özgüven, "Fabric defect detection systems and methods—A systematic literature review," *Optik-Int. J. Light Electron Opt.*, vol. 127, no. 24, pp. 11960–11973, 2016.
[24] L. Tong, W. K. Wong, and C. K. Kwong, "Fabric defect detection for apparel industry: A nonlocal sparse representation approach," *IEEE Access*, vol. 5, pp. 5947–5964, Feb. 2017.
[25] Z. Liu, L. Yan, C. Li, Y. Dong, and G. Gao, "Fabric defect detection based on sparse representation of main local binary pattern," *Int. J. Clothing Sci. Technol.*, vol. 29, no. 3, pp. 282–293, 2017.
[26] Y. Li, W. Zhao, and J. Pan, "Deformable patterned fabric defect detection with Fisher criterion-based deep learning," *IEEE Trans. Autom. Sci. Eng.*, vol. 14, no. 2, pp. 1256–1264, Apr. 2017.
[27] T. Wang, Y. Chen, M. Qiao, and H. Snoussi, "A fast and robust convolutional neural network-based defect detection model in product quality control," *Int. J. Adv. Manuf. Technol.*, vol. 94, pp. 3465–3471, Feb. 2018.
[28] R. Ren, T. Hung, and K. C. Tan, "A generic deep-learning-based approach for automated surface inspection," *IEEE Trans. Cybern.*, vol. 48, no. 3, pp. 929–940, Mar. 2018.
[29] C.-F. J. Kuo, C.-T. M. Hsu, W.-H. Chen, and C. H. Chiu, "Automatic detection system for printed fabric defects," *Textile Res. J.*, vol. 82, no. 6, pp. 591–601, 2012.
[30] G. Zhang, Z. Yuan, and N. Zheng, "Key object discovery and tracking based on context-aware saliency," *Int. J. Adv. Robotic Syst.*, vol. 10, no. 1, p. 15, 2013.
[31] H. He, "Saliency and depth-based unsupervised object segmentation," *IET Image Process.*, vol. 10, no. 11, pp. 893–899, Nov. 2016.
[32] S. X. Yu and D. A. Lisin, "Image compression based on visual saliency at individual scales," in *Proc. Int. Symp. Adv. Vis. Comput.*, 2009, pp. 157–166.
[33] J. Lee, J. D. Lee, and D. D. Salvucci, "A saliency-based search model: Application of the saliency map for driver-vehicle interfaces," in *Proc. Hum. Factors Ergonom. Soc. Annu. Meeting*, 2013, pp. 1933–1937.
[34] L. Lin and W. Zhou, "LGOH-based discriminant centre-surround saliency detection," *Int. J. Adv. Robot. Syst.*, vol. 10, no. 11, p. 385, 2013.
[35] S. Guan, "Fabric defect detection using an integrated model of bottom-up and top-down visual attention," *J. Textile Inst.*, vol. 107, no. 2, pp. 215–224, 2015.
[36] L. Itti, C. Koch, and E. Niebur, "A model of saliency-based visual attention for rapid scene analysis," *IEEE Trans. Pattern Anal. Mach. Intell.*, vol. 20, no. 11, pp. 1254–1259, Nov. 1998.
[37] X. Hou and L. Zhang, "Saliency detection: A spectral residual approach," in *Proc. IEEE Conf. Comput. Vis. Pattern Recognit.*, Jul. 2007, pp. 1–8.
[38] S. Guan and Z. Gao, "Fabric defect image segmentation based on the visual attention mechanism of the wavelet domain," *Textile Res. J.*, vol. 84, no. 10, pp. 1018–1033, 2014.
[39] Z. Liu, C. Li, Q. Zhao, L. Liao, and Y. Dong, "A fabric defect detection algorithm via context-based local texture saliency analysis," *Int. J. Clothing Sci. Technol.*, vol. 27, no. 5, pp. 738–750, 2015.
[40] S. Liu, Y. Jiang, and H. Luo, "Attention-aware color theme extraction for fabric images," *Textile Res. J.*, vol. 88, no. 5, pp. 552–565, 2018.
[41] S. Goferman, L. Zelnik-Manor, and A. Tal, "Context-aware saliency detection," *IEEE Trans. Pattern Anal. Mach. Intell.*, vol. 34, no. 10, pp. 1915–1926, Oct. 2012.
[42] J. Jing, S. Liu, P. Li, and L. Zhang, "The fabric defect detection based on CIE L*a*b* color space using 2-D Gabor filter," *J. Textile Inst.*, vol. 107, no. 10, pp. 1305–1313, 2016.
[43] T. Lei, X. Jia, Y. Zhang, L. He, H. Meng, and A. K. Nandi, "Significantly fast and robust fuzzy C-means clustering algorithm based on morphological reconstruction and membership filtering," *IEEE Trans. Fuzzy Syst.*, to be published.

[44] T. Lei, Y. Zhang, Y. Wang, S. Liu, and Z. Guo, "A conditionally invariant mathematical morphological framework for color images," *Inf. Sci.*, vol. 387, pp. 34–52, May 2017.
[45] G. Gao, D. Zhang, C. Li, Z. Liu, and Q. Liu, "A novel patterned fabric defect detection algorithm based on GHOG and low-rank recovery," in *Proc. 13th IEEE Int. Conf. Signal Process.*, Nov. 2016, pp. 1118–1123.
[46] J. Cao, J. Zhang, Z. Wen, N. Wang, and X. Liu, "Fabric defect inspection using prior knowledge guided least squares regression," *Multimedia Tools Appl.*, vol. 76, no. 3, pp. 4141–4157, 2017.
[47] H. Wang, F. Nie, and H. Huang, "Multi-view clustering and feature learning via structured sparsity," in *Proc. Int. Conf. Mach. Learn.*, 2013, pp. 352–360.
[48] H. Takeda, S. Farsiu, and P. Milanfar, "Kernel regression for image processing and reconstruction," *IEEE Trans. Image Process.*, vol. 16, no. 2, pp. 349–366, Feb. 2007.
[49] S. Liu, L. Li, Y. Peng, G. Qiu, and T. Lei, "Improved sparse representation method for image classification," *IET Comput. Vis.*, vol. 11, no. 4, pp. 319–330, Jun. 2017.

KAIBING ZHANG received the M.Sc. degree in computer software and theory from Xihua University, Chengdu, China, in 2005, and the Ph.D. degree in pattern recognition and intelligent system from Xidian University, Xi'an, China, in 2012, respectively. He is currently a Distinguished Professor at the College of Electrics and Information, Xi'an Polytechnic University, Xi'an. His main research interests include pattern recognition, computer vision, and image super-resolution reconstruction. In these areas, he has published around 20 technical articles in refereed journals and proceedings, including IEEE TIP, IEEE TNNLS, *Signal Processing* (Elsevier), *Neurocomputing*, CVPR, and ICIP.

YADI YAN received the B.Sc. degree in measurement and control technology and instruments from Xi'an Polytechnic University, Xi'an, China, in 2011, where she is currently pursuing the M.S. degree at the College of Electrics and Information. Her main research interest is computer vision and image processing.

PENGFEI LI is currently a Tertiary Professor at Xi'an Polytechnic University, Xi'an, China. His main research interests include complex textile appearance image analysis and evaluation, and textile printing and dyeing equipment intelligent detection and control system.

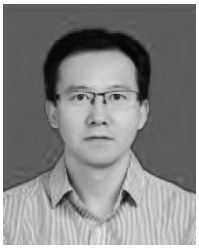

JUNFENG JING is currently a Professor at the College of Electrics and Information, Xi'an Polytechnic University, Xi'an, China. His main research interests include artificial intelligence, machine vision, image processing, and pattern recognition.

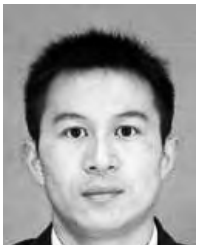

XIUPING LIU received the M.Sc. degree in system engineering from the Xi'an University of Architecture and Technology, Xi'an, China, in 2005, and the Ph.D. degree in instrument measuring technology from Xidian University, Xi'an, in 2014. Since 2014, he has been with the College of Electrics and Information, Xi'an Polytechnic University, Xi'an. His main research interests include visual tracking and virtual reality.

ZHEN WANG received the B.Sc. degree in communication engineering from Xi'an Polytechnic University, Xi'an, China, in 2016, where she is currently pursuing the M.S. degree with the College of Electrics and Information. Her main research interest is machine learning and image super-resolution reconstruction.